VOLUME 1, 2018
DOI: 10.31058/j.ac.2018.12005

Preparation and Spectral Properties of Graphene-Porphyrin Composites

Hui Lin[1], Ya Hong Wu[1], Shan Ling Tong[1], Sheng Hu[1], Heng De Li[1], Chuan Yi Pan[1], Yan Yan[1*]

[1] College of Chemical Engineering & Light industry, Guangdong University of Technology, Guangzhou, China

Email Address

yanyan600716@hotmail.com (Yan Yan)
*Correspondence: yanyan600716@hotmail.com

Received: 26 July 2018**; Accepted:** 16 October 2018**; Published:** 22 November 2018

Abstract:

Using as reactants, 4-chlorobenzaldehyde and 4-dimethylaminobenzaldehyde were selected to react with pyrrole respectively by conventional synthetic method to prepare two metal free porphyrins with peripherally substituted phenyl possessing different electronic and steric effects. The obtained *meso*-tetra (*p*-chlorophenyl) porphyrin (H_2TClPP, compound I), *meso*-tetra (*p*-dimethylaminophenyl) porphyrin (H_2TDMAPP, compound IV) and their relative Fe(III), Mn(II) complexes II, III, V and VI were characterized by spectral determinations, including UV-Vis, infrared, fluorescence, ^{1}H NMR methods. Meanwhile, the reduced graphene oxide (RGO) was prepared from crystalline flake graphite by redox method previously reported. Then the metalloporphyrin complexes II, III, V and VI were selected as candidates to composite with reduced oxidative graphene by supersonic method, and the prepared products were well characterized by UV-Vis, infrared, fluorescence, and XRD determinations. Comparing determination results indicated that all the analytic spectra displayed much different from each other. As conclusion, the metalloporphyrin-graphene composites were judged to be constructed together mainly by the weak π-π interactions with both parallel and vertical orientation. Additionally, the supplementary axial ligation between metalloporphyrin-graphene and metalloporphyrin molecules also can't be neglected in molecular assembly. According to the spectral determination results, the layered construction diagrammatic sketch of the metalloporphyrin-graphene composites was summarized in the end. Porphyrins and their complexes with planar molecule configuration displayed more attractive research attention based on their photo/electric/magnetic properties, and they were broadly applied in many research and application areas, including catalysis, molecular wires, photodynamic therapy, and photoelectric conversion. So far graphene derivatives were known as the thinnest nanomaterials with excellent stability, perfect molecular configuration, moderately molecular flexility, and outstanding conductivity. These prepared metalloporphyrin-graphene composites with prominent function, such as sensitive dyes with photoelectric transformation efficiency, were expected to be applied in assembly of dye sensitized solar cells as optically permeable electrode. This environment-friendly power sources without any pollutant emitting was mainly development purpose around the world.

DOI: 10.31058/j.ac.2018.12005

Keywords:
Porphyrin Derivative, Graphene, Composite, Spectral Characterization

1. Introduction

Metalloporphyrins with special functionality can be applied in research areas of semiconductors, [1] antineoplastic intermediates,[2] and catalytic oxidation of various hydrocarbon compounds in mimic biological enzyme reactions. [3] Axial coordination of metalloporphyrins modulated the redox potential for increasing their catalytic activities; [4,5] and peripheral halogenation around metalloporphyrins made them more stable to resist oxidation decomposition in catalytic reactions of hydrocarbon compounds. [6,7] Meanwhile graphenes attracted more research attention owing to their magical molecular configuration with excellent performance. [8-10] Moreover, the composites of metalloporphyrin-graphene were marvelous material in molecular assembly to construct molecular devices. [11,12] For investigating novel properties of porphyrin-graphene composites, several porphyrin derivatives were obtained by conventional and improved method, and these purpose compounds were physically mixed with graphemes to form the composites, followed by spectral determinations to discover their functionality. The synthesis of porphyrins and their complexes was described in Figure 1. The selected metal free porphyrin molecules with different substituents in the peripheral phenyls, one with electron acceptors, chlorine substituted groups (Compound I) and the other with electron donors, dimethylamino groups (Compound IV), and the dimethylamino groups were easy to be protonized during molecular assembly.

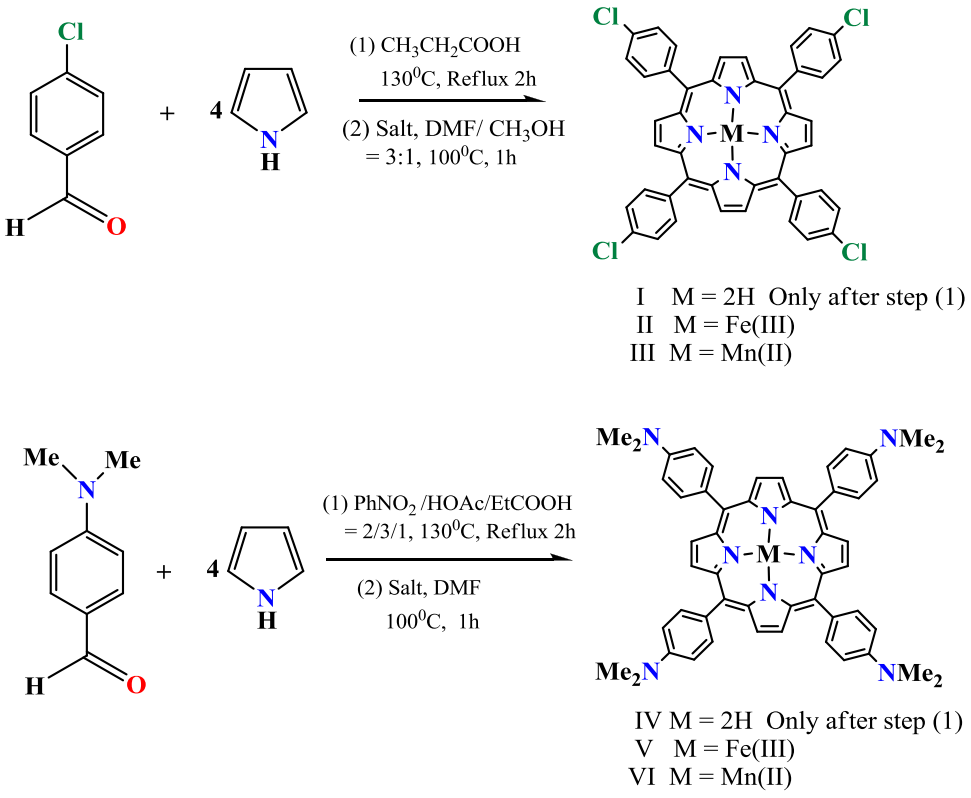

Figure 1. *Synthetic routes of porphyrins and their relative complexes.*

2. Materials and Methods

2.1. Reagents and Instrument

In porphyrin synthesis, pyrrole was used after redistillation. Other reagents were directly used as received. Fourier transform infrared (FTIR) spectra were recorded on an Avatar370FT-IR spectrophotometer (Thermo Nicolet, USA); Photoluminescence determinations were carried out on a Fluoro Max-4 fluorescence spectrometer (HORIBA Jobin Yvon, USA). The ultraviolet-visible (UV-Vis) spectra were measured by a Shimadzu UV-2450 spectrophotometer. ^{1}H NMR spectra were recorded with a Varian Mercury-Plus 300 FT-NMR (300 MHz) spectrometer in chloroform-*d* with tetramethylsilane (Me_4Si) as an internal standard. Chemical shifts (δ) and coupling constants (J) are given in parts per million and hertz respectively.

2.2. General

All hypertext links and section bookmarks will be removed from articles during the processing of articles for publication. If you need to refer to an Internet email address or URL in your articles, you must type out the address or URL fully in Regular font.

meso-Tetra (*p*-chlorophenyl) porphyrin (H_2TClPP, compound I) was synthesized according to the literature method [13,14]. Its complexes II and III with central metals of Fe(III) and Mn(II) were prepared as described in Figure 1. *meso*-Tetra (*p*-dimethylaminophenyl) porphyrin (H_2TDMAPP, compound IV) was synthesized by an improved route in a mixed solution (Figure 1), and its derivatives V and VI coordinated with Fe(III) and Mn(II) were also prepared respectively.

^{1}H-NMR (300 MHz, $CDCl_3$) δ/ppm for H_2TClPP, compound I: -2.943 (s, 2H, H-N in pyrrole); 7.775 (t, J = 3 Hz, 8H, *m*-H in phenyl), 7.89ppm-8.365ppm (d, J = 8.4 Hz, 8H, *o*-H in phenyl), 8.831 (s, 8H, β-H in pyrrole); IR (KBr)/cm^{-1} for compound I: 3440.44 ($\nu_{N\text{-}H}$, pyrrole); 1653.34, 1488.63 ($\nu_{C=C}$, phenyl); 1394.33($\nu_{C=N}$, pyrrole); 799.85($\delta_{N\text{-}H}$, pyrrole); 799.85 (character vibration of p-substituted phenyl), 786.24($\nu_{C\text{-}Cl}$, *p*-Cl in phenyl). For Complex II: 1635.53, 1457.10 ($\nu_{C=C}$, phenyl); 1389.66 ($\nu_{C=C}$, pyrrole); 803.90 (character vibration of *p*-substituted phenyl), 771.11 ($\nu_{C\text{-}Cl}$, *p*-Cl in phenyl). For Complex III: 1627.28, 1485.50 ($\nu_{C=C}$, phenyl); 1389.66 ($\nu_{C=N}$, pyrrole); 801.94 (character vibration of p-substituted phenyl), 770.12 ($\nu_{C\text{-}Cl}$, *p*-Cl in phenyl). ^{1}H-NMR (300 MHz, $CDCl_3$) δ/ppm for H_2TDMAPP, compound IV: -2.984 (s, 2H, H-N in pyrrole); 2.311 (s, 24H, -NMe_2); 7.721 (t, J = 3 Hz, 8H, *m*-H in phenyl); 8.362 (t, J = 8.3 Hz, 8H, *o*-H in phenyl); 8.832 (s, 8H, β-H in pyrrole). IR (KBr)/cm^{-1} for compound IV: 2922.51 ($\nu_{C\text{-}H}$ in -NMe_2); 1608.36, 1525.8 ($\nu_{C=C}$, phenyl); 1346.79 ($\nu_{C=N}$, pyrrole); 945.29 ($\delta_{N\text{-}H}$, pyrrole); 802.29 (character vibration of *p*-substituted phenyl). For Complex V: 2911.25 ($\nu_{C\text{-}H}$ in –NMe_2); 1604.10, 1496.43 ($\nu_{C=C}$, phenyl); 1348.29 ($\nu_{C=N}$, pyrrole); 804.50 (character vibration of *p*-substituted phenyl). For Complex VI: 292.83 ($\nu_{C\text{-}H}$ in –NMe_2); 1608.14, 1518.40 ($\nu_{C=C}$, phenyl); 1349.81 ($\nu_{C=N}$, pyrrole); 802.46 (character vibration of *p*-substituted phenyl).

3. Results and Discussion

3.1. UV-Vis Analysis of Meso-Substitutedphenyl Porphyrins and Their Complexes

UV-Vis spectra of H_2TClPP (Compound I) and its complexes with Fe^{III} and Mn^{III}

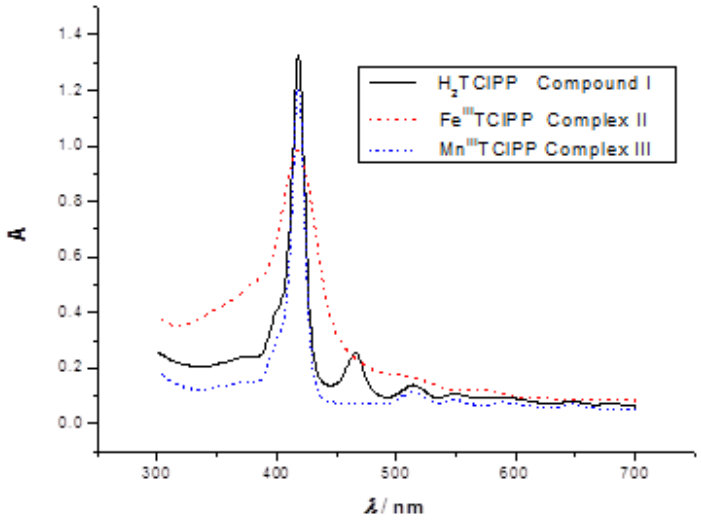

Figure 2A

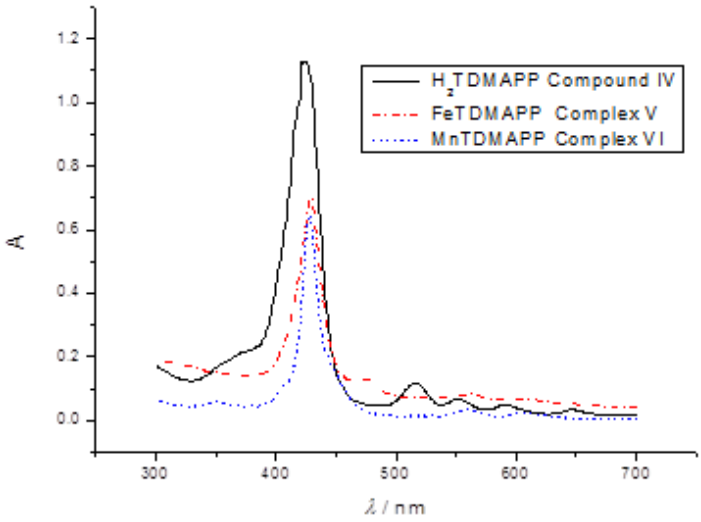

Figure 2B

Figure 2. *A. The UV-Vis spectra of H2TClPP (Compound I) and its complexes with FeIII and MnIII (Complexes II and III) in DMF (1.0 10-3 mol/L) B. The UV-Vis spectra of H2TDAMPP (Compound IV) and its complexes with FeIII and MnIII (Complexes V and VI) in DMF (1.0 10-3 mol/L).*

(Complexes II and III) in DMF were recorded in Figure 2A. Compound I displayed one Soret peak at 418 nm (ε_{max} = 1.58×10^6 L mol^{-1} cm^{-1}) and four Q peaks at 466, 514, 549 and 647 nm (ε_{max} = 2.68×10^5, 1.34×10^5, 9.7×10^4 and 6.2×10^4 L mol^{-1} cm^{-1}). After coordination with central metals, the shapes and positions of Complexes II and III have changed clearly. For Complexes II, its Soret peak at 418 nm was weakened and broadened; meanwhile its Q bands were reduced to two peaks at 505 and 569 nm. For Complex III, its spectra was similar to that of Compound I, excepting disappearance of Q band at 466 nm.

UV-Vis spectra of H_2TDAMPP (Compound IV) and its complexes with Fe^{III} and Mn^{III} (Complexes V and VI) in DMF were given in Figure 2B. Compound IV presented one Soret peak at 425 nm (ε_{max} = 1.33×10^6 L mol^{-1} cm^{-1}) and four Q peaks at 515, 552, 591 and 646 nm (ε_{max} = 1.15×10^5, 6.0×10^4, 4.0×10^4 and 2.7×10^4 L mol^{-1} cm^{-1}). After complex formation, their UV-Vis spectra changed clearly. For Complexes V and VI, their Soret peaks appeared at 429 and 428 nm with slightly red-shift. Meanwhile, their Q peak numbers reduced and Q peak position were changed clearly with much different from Compound IV. The UV-Vis spectral evidences indicated the purpose metalloporphyrins were successfully prepared.

3.2. Emission Spectra of Meso-Substitutedphenyl Porphyrins and Their Complexes

The emission spectra for H_2TClPP (Compound I) and its complexes with Fe^{III} and Mn^{III}(Complexes II and III) were given in Figure 3A. Compound I presented one strong emission peak at 656nm and one weak peak at 714 nm. Its complexes of Fe and Mn (Complexes II and III) also exhibited two emission peaks with blue shift, the strong peaks for Complexes II and III appeared at 649 and 654 nm, but the weak peaks at 714 nm were without clear change in positions. After complex formation, the emission spectra possessed clear fluorescence quenching.

Figure 3B was the compared emission spectra for H_2TDMAPP (Compound IV) and its complexes with Fe^{III} and Mn^{III}(Complexes V and VI). There were two emission peaks detected in their FL spectra. For Compound IV one strong emission peak appeared at 651 nm and one weak peak at 716 nm. The emission spectra of Fe and Mn complexes (Complexes V and VI) also exhibited two emission peaks without any blue shift, but with clear fluorescence quenching.

3.3. Characterization of Graphene-Metalloporphyrin Composites

According the mentioned method, the composites of graphene-metalloporphyrins were prepared and separated. Figure 4 showed the UV-Vis spectra of reduced graphene oxide (grapheme, GR), metalloporphyrins and their composites. Figure 4A showed a broad peak around 250 nm for GR from the -plasmon, [15, 16] without any absorption in the visible light region, indicating the graphene oxide was conversed completely into the reduced form. After compositing with metalloporphyrins, the obtained composite material showed different behavior in the spectra. For GR-Complex II (Figure 4A), the broad peak for GR was become a weak peak at 318 nm with clear red shift, and appeared at 409 nm (Soret band, with blue shift, 9nm); 569 nm (enhanced Qband) and 609nm (Q band); the original Q band for Complex II at 505 nm was difficultly observed. The situation for GR-Complex V was similar to the above statement (Figure 4C). In the spectrum of GR-Complex V, the broad peak for GR was split into two peaks at 313 nm and 364 nm. Soret band appeared at 425 nm (with 4 nm blue shift than Complex V), and two Q bands appeared at 519 nm and 565nm, which were much different from ones of Complex V.

The UV-Vis spectra for MnPorphyrin-graphene composites (Figure 4B and 4D) were much different from those of GR and metalloporphyrin. Excepting peak vanishing at 250nm for GR, metalloporphyrin's characteristic peaks was changed extensively. The composite of GR-Complex III (Figure 4B) presented a Soret band at 467 nm (for Complex III the peak located at 418nm) with 49 nm red shift. Its Q bands were detected at 568 and 602 nm with clear red shift, too. For composite of GR-Complex VI (Figure 4D), the Soret band appeared at 465 nm (with 37 nm red shift

than that of Complex VI), but two Q bands nearly kept changeless. The change of shapes and positions in UV-Vis spectra indicated that novel porphyhrin species produced.

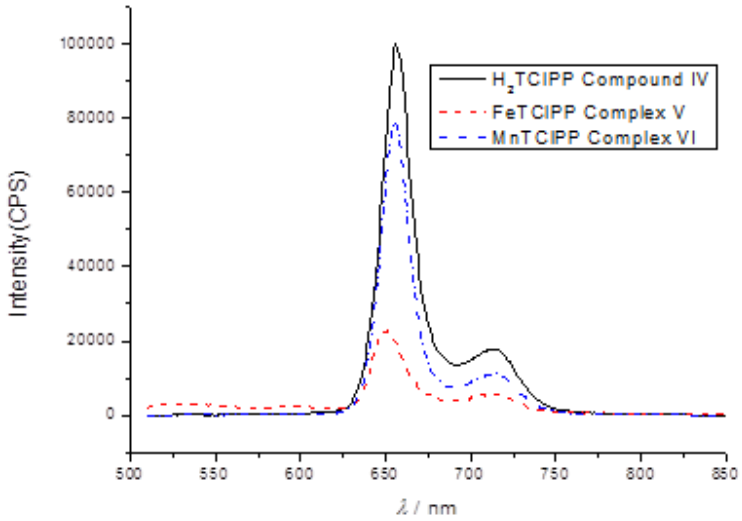

Figure 3A

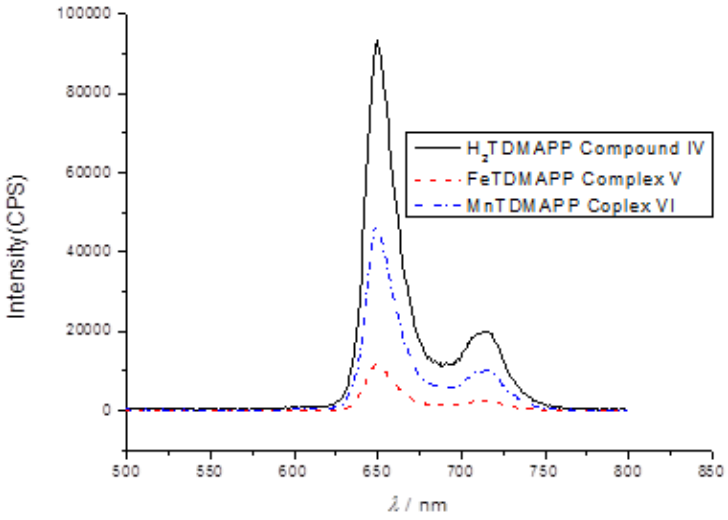

Figure 3B

Figure 3. *A. The emission spectra of H2TClPP (Compound I) and its complexes with FeIII and MnIII (Complexes II and III) in DMF (1.0×10-4 mol/L, λEX = 436 nm) B. The emission spectra of H2TDMAPP (Compound IV) and its complexes with FeIII and MnIII (Complexes V and VI) in DMF (1.0×10-4 mol/L, λEX = 440 nm).*

This clearly red shift for Mn-porphyrin-graphene composites (Figure 4B and Figure 4D) indicated that the electron transfer energy reduction, and if this material was assembled as electrode in dye sensitized solar cell, the long wave light would be efficiently absorbed to transfer as electric energy. Therefore the optical capture efficiency for porphyrin-graphene composites can be improved by changing central

metal of the metalloporphyrins. The Soret band red shift and Q band enhancement were beneficial for optical capture.

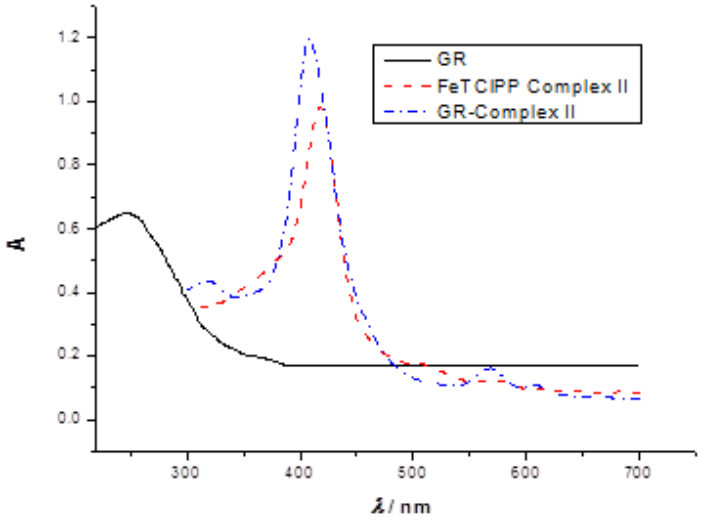

Figure 4A

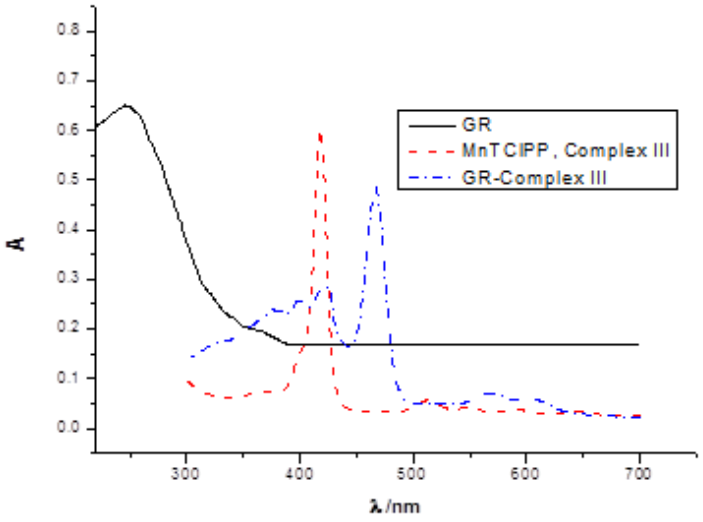

Figure 4B

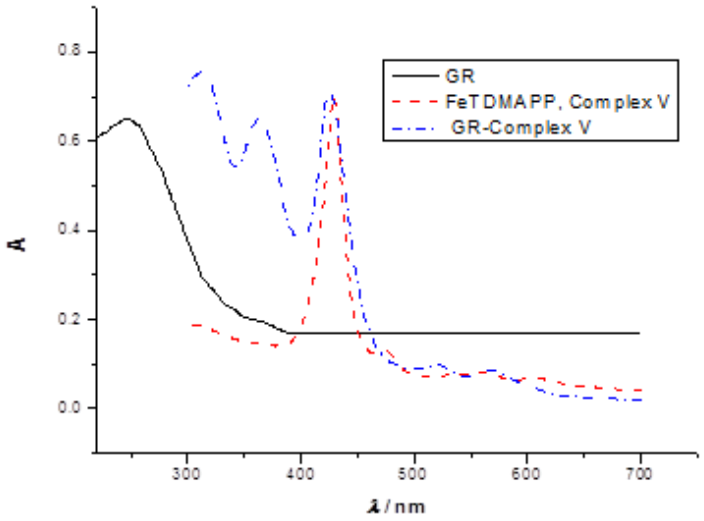

Figure 4C

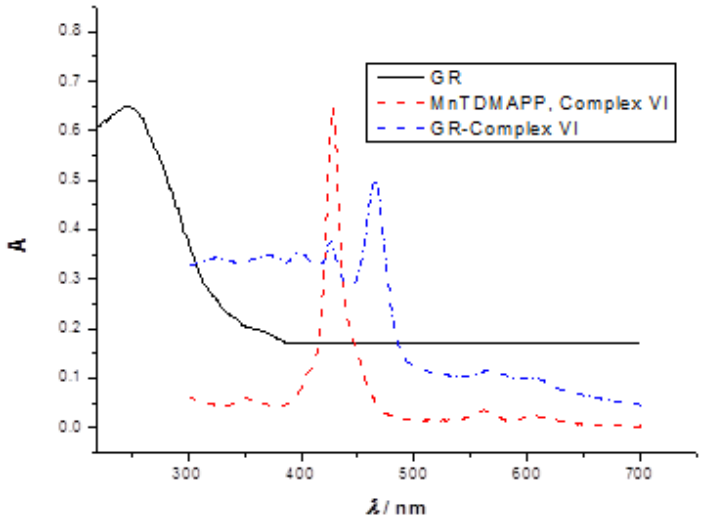

Figure 4D

Figure 4. *The UV-Vis spectra of graphene (GR), metalloporphyrins, and composites of GR-metalloporphyrins. A. FeTClPP, Complex II; B. MnTClPP, Complex III; C. FeTDMAPP, Complex V; D. MnTDMAPP, Complex VI.*

Figure 5 was the comparing fluorescence spectra of metalloporphyrins and their composites with graphene. The photoluminencence of metalloporphyrin-graphene composites were similar to those of Complexes II and VI (Figure 5A and 5D). But the FL spectra of the composites of Complexes III and V were much different form ones of Complexes III and V themselves. For MnTClPP-GR, excepting peaks at 651 and 714 nm, a new peak appeared at 605 nm (Figure 5B); and for FeTDMAPP-GR, new FL peaks at 618 and 659 nm exhibited clearly red shift effects. These results meant photoluminescence energy decreasing for the Fe-porpyrin composites, and for Mn-porphyrin composites were also with clear red shift in their FL spectra, indicating their photoluminescence energy decreasing. Different central metals resulted in different photoluminescent effects. These observed FL

changes exhibited that the interactions between porphyrin and graphene were complicated, including weak - stacking, axial coordination and some unclear physically and chemically structural forces. In the composites, the weak interactions changed the original shapes for both graphene and metalloporphyrin configurations and resulted in clear FL changes.

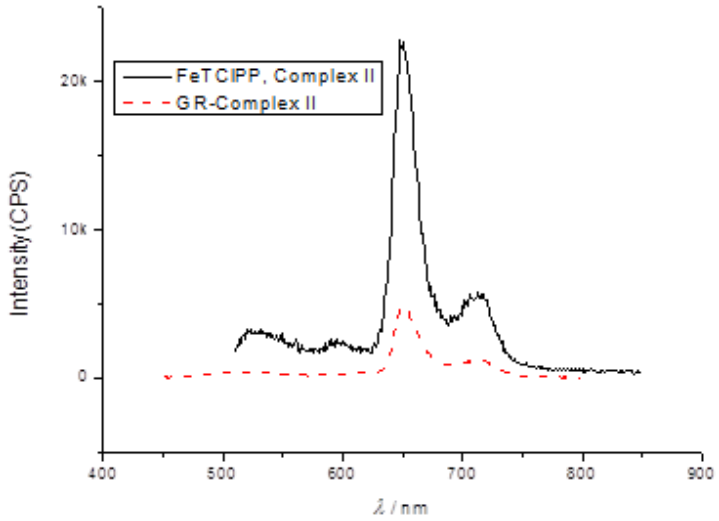

Figure 5A

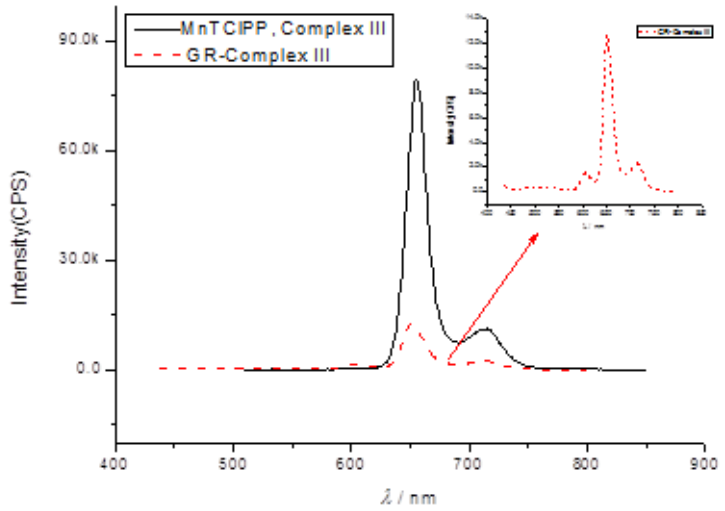

Figure 5B

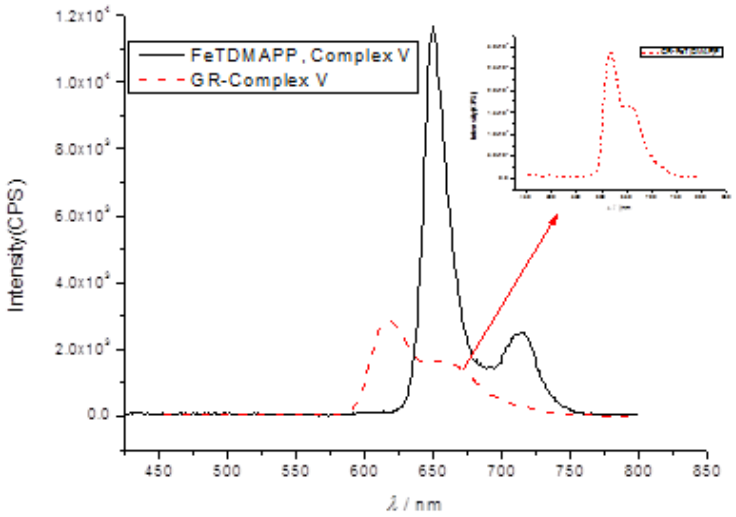

Figure 5C

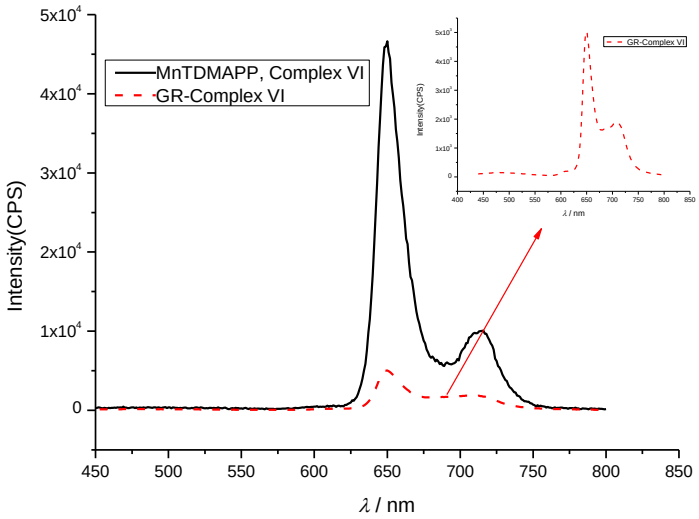

Figure 5D

Figure 5. *The comparing fluorescence spectra of metalloporphyrins and their composites with graphene. A. Complex II and GR composite; B. Complex III and GR composite; C. Complex V and GR composite; D. Complex VI and GR composite.*

XRD determination results for the metalloporphyrin-graphene composites were given in Figure 6. Comparing with GR and metalloporphyrin, the composites displayed well crystal properties, the broad diffusion peaks of GR was disappeared, and the characteristic diffusion peaks of metalloporphrins were enhanced. The sharp diffusion peak in GR was also disappeared for GR composites of Complexes II, V and VI. But in GR-Complexes III composites, this diffusion was remarkable enhanced. The change in XRD determinations were closely related to crystal morphology. The comparing XRD determination results also indicated the crystal property changes after composite formation.

Similar to XRD determination, IR determination results of the GR-metalloporphyrin composites showed enhancing vibration with both GR and metalloporphyrin characteristics.

Both graphene and porphyrin were flat conjugated system in their molecular configuration. Therefore the driving forces to construct the composites were judged mainly dependence on the weak - interactions. [17,18,19] Composites constructions of metalloporphyrins and RGOs were possibly as described in Figure 7. Excepting the - interactions, the peripheral substituents around porphyrin molecules, such as chlorine atoms and dimethylamino groups, supplied weak hydrogen bonding (HB) interactions with nearby hydrogen atoms. [20] These HB interactions provided the other weak forces to sustain the construction of porphyrin-graphene composites.

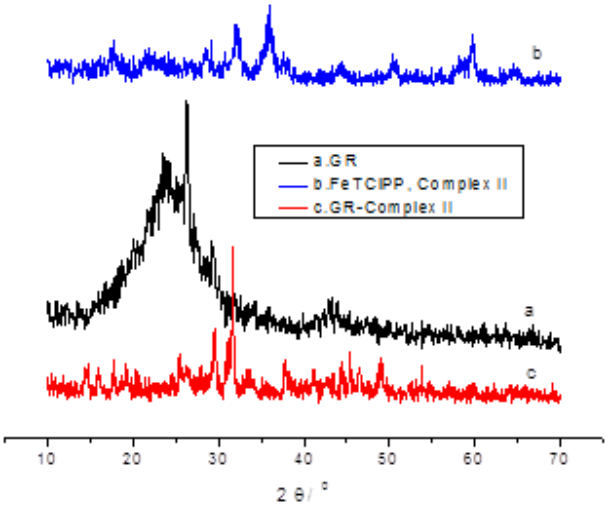

Figure 6A

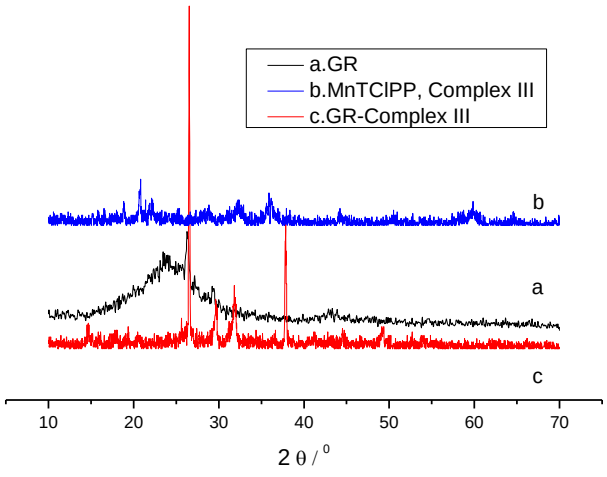

Figure 6B

DOI: 10.31058/j.ac.2018.12005

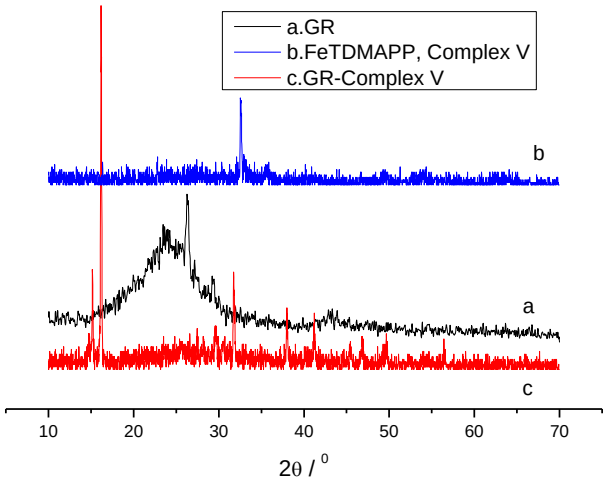

Figure 6C

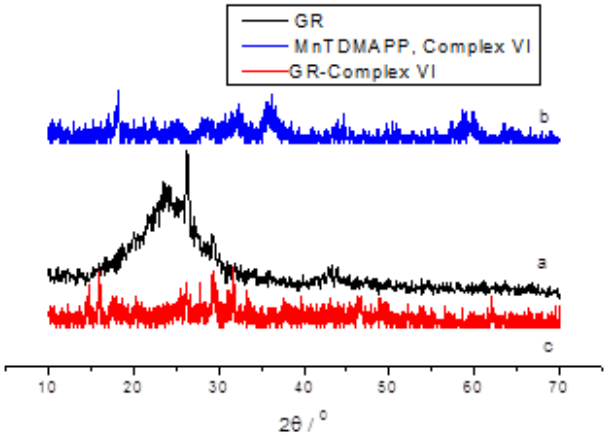

Figure 6D

Figure 6. *The comparing XRD spectra of metalloporphyrins and their composites with graphene. A. Complex II and GR composite; B. Complex III and GR composite; C. Complex V and GR composite; D. Complex VI and GR composite.*

4. Conclusions

In this paper, metalloporphyrin as interlayers were successfully inserted between graphene layers by supersonic method. Under supersonic vibration, both graphene and metalloporphyrin molecules were stretch enough into planar configuration for convenient composition of layered construction, just as littered mess paper were put together with fitly superposition.

When the conjugated molecules were effectively stretched into planar configuration, molecular resonance reached whole conjugation state. According to the analytic results from the above spectral determinations, the GR-metalloporphrin composites

were judged to be constructed mainly by weak - stacking, since both GR and metalloporphyrins displayed planar configuration with fully conjugation system, and the planar conjugation systems were easy combined together by weak intermoleclular interactions, including efficiently parallel and more weaker vertical orientation - stacking.

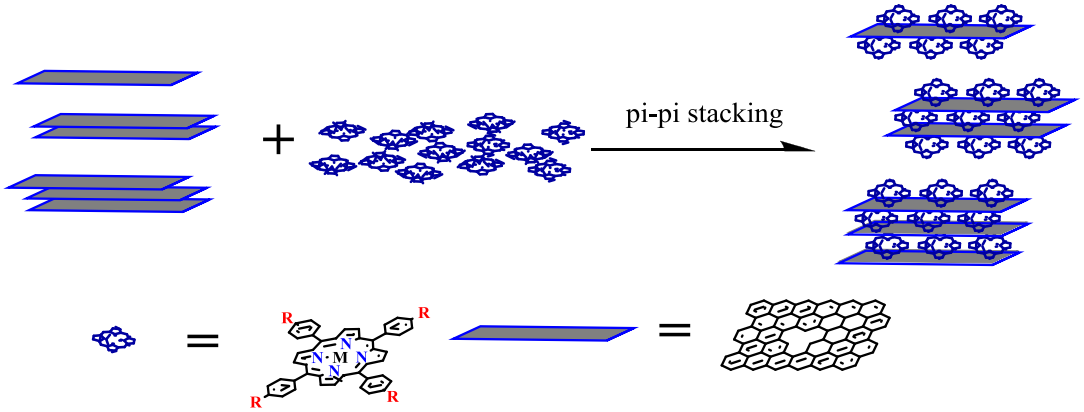

Figure 7. *Composites of RGO-metalloporphyrin with π-π stacking interacting.*

Since central metal Fe (III) and Mn (III) ion with strong static attraction towards electrons, therefore the static interactions, between graphene and metalloporphyrin molecules, and even the axial coordination between metalloporphyrin molecules, would not be ignored during composite construction. Additionally, graphene configuration was adopted mixed sp2 and sp3 hybridization with pore geometry along with epoxyl, hydroxyl and even carboxyl groups. [21,22] Although these construal characters resulted in graphene corrugating and partially destroying - stacking between metalloporphyrin and grapheme, the polarity increasing would enhance the molecular interactions between metalloporphyrin and graphene. Furthermore, the electronic and steric effects form the peripheral substituents around porphyrin rings can also influence the assembly fashion. In Compound I and the relative Complexes II and III, the chlorine groups with strong electronegativity and weak steric effects supplied strong polar actions in composition with graphene; while in Compound IV and its Complexes V and VI, the dimethylamino groups with strong steric effects can be easy protonized, and this trend may course strong electrostatic interaction during compositions. Therefore the driven forces to construct the composites involved varied intermolecular interactions.

Conflicts of Interest

The authors declare that there is no conflict of interest regarding the publication of this article.

Acknowledgments

The authors thanks for the financial supporting from the Natural Science Fund in Guangdong Province (Grant No. 2017A030313071), and from The Key Project of Education Office of Guangdong Province, China (Grant No. 2012CXZD0023).

References

[1] Hakola, H.; Perros, A. P.; Myllyperkio, P.; Kurotobi, K.; Lipsanen, H.; Imahori, H.; Lemmetyinen, H.; Tkachenko, N. V. Photo-induced electron transfer at

nanostructured semiconductor-zinc porphyrin interface. *Chem. Phys. Lett*, 2014, 592, 47-51, DOI: 10.1016/j.cplett.2013.11.028.

[2] Pinellia, A.; Mussini, C.; Buratti, M.; Parmiggiani-Venezia, M.; Trivulzio, S. Increased urinary coproporphyrin excretion observed in patients with differently staged Hodgkin's disease treated with chemotherapy. *Pharmacological Res*, 2005, 51, 283-288, DOI: 10.1016/j.phrs.2004.09.005.

[3] Mak, P. J.; Denisov, I. G. Spectroscopic studies of the cytochrome P450 reaction mechanisms. *BBA - Proteins and Proteomics*, 2018, 1866, 178-204, DOI: 10.1016/j.bbapap.2017.06.021.

[4] Chandra, B. K. C.; Francis, D. Design and photochemical study of supramolecular donor–acceptor systems assembled via metal-ligand axial coordination. *Coordin. Chem. Rev*, 2016, 322, 104-141, DOI: 10.1016/j.ccr.2016.05.012.

[5] Lee, H.; Hong, K. I.; Jang, W. D. Design and applications of molecular probes containing porphyrin derivatives. *Coordin. Chem. Rev*, 2018, 354, 46-73, DOI: 10.1016/j.ccr.2017.06.008.

[6] Lyons, J. E.; Ellis, P. E.; Myers Jr, H. K. Halogenated metalloporphyrin complexes as catalysts for selective reactions of acyclic alkanes with molecular oxygen. *J. Catal*, 1995, 155, 59-73, DOI: 10.1006/jcat.1995.1188.

[7] L ü, Q.; Yu, R.; Shen, G. The structure, catalytic activity and reaction mechanism modeling for halogenated iron-tetraphenylporphyrin complexes. *J. Mol. Catal. A: Chem*, 2003, 198, 9-22, DOI: 10.1006/S1381-1169(02)00726-4.

[8] Zhang, C.; Nicolosi, V. Graphene and MXene-based transparent conductive electrodes and supercapacitors. *Energy Storage Materials*, 2019, 16, 102-125, DOI: 10.1016/j.ensm.2018.05.003.

[9] Lim, J. Y.; Mubarak, N. M.; Abdullah, E. C.; Nizamuddin, S.; Khalid, M.; Inamuddin. Recent trends in the synthesis of graphene and graphene oxide based nanomaterials for removal of heavy metals — A review, *J*

[10] Park, J.; Choa, Y. S.; Sung, S. J.; Byeon, M.; Yang, S. J.; Park, C. R. Characteristics tuning of graphene-oxide-based-graphene to various end-uses, Energy Storage Materials, 2018, 14, 8-21, DOI: 10.1016/j.ensm.2018.02.013.

[11] Aradhana, D. M.; Dissanayake, S.; Cifuentes, M. P.; Humphrey, M. G. Optical limiting properties of (reduced) graphene oxide covalently functionalized by coordination complexes. *Coord. Chem. Rev*, 2018, 375, 489-513, DOI: 10.1016/j.ccr.2018.05.003.

[12] Wu, H.; Li, X.; Chen, M.; Wang, C.; Wei, T.; Zhang, H.; Fan, S. A nanohybrid based on porphyrin dye functionalized graphene oxide for the application in non-enzymatic electrochemical sensor. *Electrochimica Acta*, 2018, 259, 355-364, DOI: 10.1016/j.electacta.2017.10.122.

[13] Adler, A. D.; Longo, F. R.; Kampas, F.; Kim, J. On the preparation of metalloporphyrins. *J. Inorg. Nucl. Chem*, 1970, 32, 2443-2445, DOI: 10.1016/0022-1902(70)80535-8.

[14] Lindsey, J. S.; Schreiman, I. C.; Hsu, H. C.; Kearney, P. C.; Marguerettaz, A. M. Synthesis of tetraphenylporphyrins under very mild condition. *J. Org. Chem*, 1987, 52, 827-836, DOI: 10.1016/S0040-4039(00)85109-6.

[15] Wu, J.; Shen, X.; Jiang, L.; Wang, K.; Chen, K. Solvothermal synthesis and characterization of sandwich-like graphene/ZnO nanocomposites. *Appl. Surf. Sci*, 2010, 256, 2826-2834, DOI: 10.1016/j.apsusc.2009.11.034.

[16] Rance, G. A.; Marsh, D. H.; Nicholas, R. J.; Khlobystov, A. N. UV-vis absorption spectroscopy of carbon nanotubes: Relationship between the -electron plasmon and nanotube diameter. *Chem. Phys. Lett*, 2010, 493, 19-23, DOI: 10.1016/j.cplett.2010.05.012.

[17] Fan, S.; Yang, J.; Wei, T.; Zhang, J.; Zhang, N.; Chai, M.; Jin, X.; Wu, H. Zinc porphyrin–fullerene derivative noncovalently functionalized grapheme hybrid as interfacial material for electrocatalytic application. *Talanta*, 2016, 160, 713-720, DOI: 10.1016/j.talanta.2016.08.018.

[18] Ye, T.; Ye, S.; Chen, D.; Chen, Q.; Qiu, B.; Chen, X. Spectroscopic characterization of tetracationic porphyrins and their noncovalent functionalization with graphene. *Spectrochimica Acta Part A*, 2012, 86, 467-471, DOI: 10.1016/j.saa.2011.10.070.

[19] Riseviciene, R. R.; Grinceviciute, N.; Selskis, A.; Snitka, V. Synthesis ofhybridgraphene–porphyrinmicro/nanofiber structuresby ionic self-assembly. *Materials Lett*, 2016,164, 160-164, DOI: 10.1016/j.matlet.2015.10.149.

[20] Wei, Y. J.; Chun, H. X.; Bin, L. J.; Tie, C.; Jing, X.; Ling, T. S.; Er, Y. K.; Yan, Y. Crystal Structure and Catalytic Properties of Tetrakis(4-hydroxypheny1)Porphyrinato Manganese(III)Chloride(MnTHPPCI). *Chem. Res. Chinese U*, 2007, 23, 384-387, DOI: 10.1016/S1005-9040(07)60082-8.

[21] Mombru, D.; Faccio, R.; Mombru, A. W. Emulating porphyrins with a rippled multivacancy graphene system. *Appl. Surf. Sci*, 2018, 436, 1173-1180, DOI: 10.1016/j.apsusc.2017.12.162.

[22] Karachevtsev, V. A.; Stepanian, S. G.; Karachevtsev, M. V.; Adamowicz, L. Graphene induced molecular flattening of meso-5,10,15,20-tetraphenyl porphyrin: DFT calculations and molecular dynamics simulations. C*omput. Theor. Chem*, 2018, 1133, 1-6, DOI: 10.1016/j.comptc.2018.04.009.